The 2009 IEEE/RSJ International Conference on
Intelligent Robots and Systems
October 11-15, 2009 St. Louis, USA

Vibration Detection and Backlash Suppression in Machine Tools

Ebrahim Mohammadiasl

Abstract—**Mechanical backlash is a common trouble in all servo mechanisms that is created by mechanical defects i.e. wear or looseness. Backlash imposes nonlinearity on a linear control system and may be contributed to a limit cycle. Considering mechanical subsystem of a servo axis as an elastic two-mass system, modeling the backlash with a dead zone and choosing reduced order control system for the speed and current controller, the frequency bandwidth of vibration is estimated. The estimated frequency is supported by the experimental vibration analysis of six different machine tools. To eliminate unwanted vibration, a backlash detection and suppression approach is proposed in this paper. In the case of vibration, load sensor is disregarded and the regulator conducts the setting speed of interpolator to the drive. Then stability is satisfied with the cost of some tracking error. When stability is detected load sensor is considered and the regulator output converges to the speed provided by the position control. To examine the approach, dynamic model of a real servo axis is obtained and it is validated by experimental data. Then the proposed modified control system is simulated.**

Keywords—*Backlash, machine tools, Vibration, Regulator.*

I. Introduction

Backlash causes inaccurate motion, and extraordinary vibration which imposes severe limitations on the quality of control. Mechanical backlash comprises two different phenomenas: impact and free play. To account the impact behavior(that dominates motion at low amplitude), the contact force is considered and dynamic model of mechanical backlash is derived[1-2-3]. In the control system literature backlash is modeled as a free play with pure plastic impact or free play with linear elastic contact(Dead zone) and describing function is used to predict limit cycle[4-5]. Frequency of vibration caused by backlash is estimated by using high stiff impact model[6]. And in the case of considerable inner damping coefficient, the exact model of viscoelastic mechanism(backlash included) is recommended[7]. According to the literature survey, backlash suppression problem is a trade off between procuring fast response system and robust control. Various techniques suggested for backlash suppression have been studied in the survey papers[8-9]. Linear PI/PID like speed controller and nonlinear, advanced approaches have been conducted to solve the problem of vibration in mechanical subsystems[10 to 17]. In the case of known backlash, a backlash compensating controller can guarantee exact positioning. And by calculating time interval between each contact of driver and driven parts, impact can be dampened[18]. Also several approaches have been offered for backlash detection and estimation[19-20].

In this paper, first, the reduced order model of mechanical system of a servo axis is introduced, and an ordinary cascade control system is reviewed. Next, the frequency bandwidth of vibration caused by backlash is estimated. The estimated frequency is backed up with the experimental vibration taken from six mechanically different servo axes. Then to maintain the stability and the exactness, a vibration detection algorithm is proposed and a specific speed regulator is designed. The validated model of a real servo axis is used and the application of proposed control system is simulated where the performance and the advantages are clarified.

Manuscript received February 27, 2009. Vibration Detection and Backlash Suppression in Machine Tools.

Ebrahim Mohammadiasl is with the Maintenance Department of Mapnaturbine Manufacturing Co.(TUGA), Karaj, IRAN (e-mail: emohammadi@mapnaturbine.com; ebmohammadi@yahoo.com).

II. Servo Axes and Measuring Systems

A. Axis Types

Generally, industrial machine tools include two types of axes: machining-contour axes and positioning axes. Contour axes implemented for machining operation while positioning axes i.e. indexing table are involved for orientation of a workpiece. Machining axes are guided by an interpolator which defines the contour points such that all axes start the motion(and stop at the programmed target point) simultaneously. For this reason interpolating machining axes must have the identical dynamic behavior i.e. the same following error for the same acquired speed. With the equal position gain for all machining axes the expected following error would be the same:

$$Following\_error = Command\_speed / Position\_gain(k_v) \quad (1)$$

In comparison, a positioning axis traverses independently and for this axis stand still positioning(not dynamic tracking error) is of most interest.

B. Measuring Systems

Usually, both the machining and positioning axes are equipped with two encoders that are known as motor measuring system(motor encoder-sensor), and direct measuring system(load sensor). The load sensor is directly connected to the axis and provides the exact positioning signal(is not affected by backlash) of the axis(tool) to high level position controller. The motor encoder signal is used as a feedback for speed controller. And to assure the safe motion of machine tools, measured position by the motor

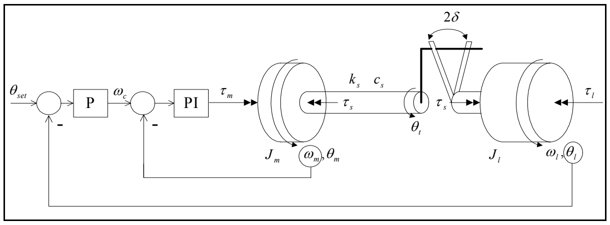

Fig. 1. Simple model of a servo axis

and direct encoder should be in a limited tolerance(about 0.5mm or 0.5deg). This limited difference between two measuring systems is defined based on the stiffness and accuracy of mechanical parts, installing condition, temperature variation and etc. So the difference between two measuring systems is not practical to detect backlash(especially in the case of high ratio transmission).

III. Mechanical subsystem

Mechanical part like gear, lead screw, compliant coupling, etc. can be modeled as a set of spring and damper, and the more mechanical components we have the more resonance frequencies will be resulted. However, to avoid mathematical complication, a servo axis is modeled based on one dominant resonance frequency, and the other elements assumed to behave rigidly. Fig.1 shows the schematic model of an ordinary servo axis and the corresponding symbols are presented in Table I.

A compliant coupling between motor and load doubles the number of state variables within the mechanical subsystem. In fact, speed and position of the motor differ from the respective variables on the load side and low damping coefficient gives rise to mechanical oscillation. Transfer functions of the mechanical subsystem based on the motor and load sensor($W_m = \omega_m / \tau_m$, $W_l = \omega_l / \tau_m$) and transmission ratio of one($k_r = 1$) are given in (2), (3):

$$W_m = \frac{1}{(J_m + J_l)s} \frac{P}{Q} \tag{2}$$

$$W_l = \frac{1}{(J_m + J_l)s} \frac{P_a}{Q} \tag{3}$$

Where resonance and anti-resonance frequencies(ω_r, ω_a), relative damping ratios(ξ_r, ξ_a), P, P_a and Q are given by:

$\omega_a = \sqrt{k_s / J_l}$, $\omega_r = \sqrt{k_s (1/J_m + 1/J_l)}$, $\xi_a = c_s \omega_a / (2k_s)$, $\xi_r = c_s \omega_r / (2k_s)$, $P = 1 + 2\xi_a (s/\omega_a) + (s/\omega_a)^2$, $P_a = 1 + 2\xi_a (s/\omega_a)$, $Q = 1 + 2\xi_r (s/\omega_r) + (s/\omega_r)^2$.

In a servo system with a gearbox, where elastic element assumed to be at the load side the stiffness, load inertia and damping ratio should be replaced with their reflected values(k'_s, J'_l, $\xi'_{a,r}$) in (2) and (3) as:

$J'_l = J_l / k_r^2$, $k'_s = k_s / k_r^2$, $\omega'_r = \sqrt{k'_s (1/J_m + 1/J'_l)}$, $\omega'_a = \sqrt{k'_s / J'_l} = \omega_a$, $\xi'_a = \xi_a$, $\xi'_r = c_s \omega'_r / (2k_s)$.

TABLE I
Symbols and Definition

Symbol	Defination
τ_l	load torque
τ_s	torsion torque
τ_m	motor torque
τ_f	friction torque
J_m	motor moment of inertia including coupling
J_l	load moment of inertia
θ_m	motor angle(motor sensor)
θ_l	load angle(load sensor)
ω_s	speed reference point of interpolator
ω_c	speed set point of drive(speed controller)
ω_m	motor speed(motor sensor)
ω_l	load speed(load sensor)
e_l	following error of load(direct measuring system)
k_s	stiffness(compliance) of axis
c_s	damping of impact
c_m	damping of motor shaft
c_l	damping of load side
k_r	ratio between motor speed and axis speed
δ	backlash (reflected on load-tool side)
k_v	position control gain
k_{sp}	speed controller proportional gain
T_{si}	speed controller integrator time

Two other important parameters, namely inertia ratio(R) and resonance ratio(H), are defined by (4).

$$R = J_l / J_m, \; H = \omega_r / \omega_a = \sqrt{1+R} \tag{4}$$

The first term in the right side of (2) and (3) manifestoes the rigidly-coupled motor and load, and the next terms show the effect of compliance. When the load speed is conducted to the speed controller mechanical resonator is included in the loop control that decreases bandwidth frequency of the control system. In contrast, motor encoder provides exact position of motor shaft and excludes motor-load compliance. In this case with a lower value of inertia ratio($J_l << J_m$), oscillation of torsion torque is filtered by the large motor inertia, and the load vibration does not influence the dynamic of speed controller. However, even with a stiff control over the motor speed, the load speed will face with low damped oscillation. For the applications like machine tools where the exact positioning of the load(tool) is concerned transmissions are optimized in a way that inertia ratio became between 2 and 3 and mostly less than 5. It was shown that optimum value for inertia ratio is 2.2[12].

IV. DESCRIBING FUNCTION

Mechanical backlash can be modeled by a dead zone and the normalized gain of sinusoidal-input describing function(SIDF) is given in nonlinear control articles:

$$N(A)=\begin{cases}1-\dfrac{2}{\pi}\left[\sin^{-1}\left(\dfrac{\delta}{A}\right)+\dfrac{\delta}{A}\sqrt{1-\left(\dfrac{\delta}{A}\right)^2}\right] & \delta\geq A\\ 0 & \delta<A\end{cases} \tag{5}$$

Where $N(a)$ is the normalized gain of describing function, A is the amplitude of the input sinusoidal signal. In (5) dead zone is described as a function of input amplitude and is not frequency dependent(memory less function). And the effect of backlash can be seen as a gain between 0 and 1. Since δ is divided by A in (5), the shape of describing function in Nyquist graph is independent from δ. It means that the occurrence of limit cycle and the oscillation period defined in Nyquist plot is not affected by the magnitude of mechanical backlash[4-5].

V. AXIS CONTROL SYSTEMS

The controller of our investigated machine tools is common cascade type including high level "P"(proportional) position controller, "PI" speed controller and "PI" current controller where actuator is a permanent magnet synchronous motor(AC servo motor). Each inner loop in the cascade control is to be designed to provide higher cross frequency(about an order of magnitude) in respect to it's outer loop.

For tuning the servo gain of the speed and current controller an attempt should be done to keep the amplitude of closed loop speed (and current) controller at 0dB over the widest frequency bandwidth. Resonance frequencies are dampened by set point notch filters at the input of current controller. In practice, the frequency bandwidth of the current controller reaches to about 500-1000HZ[21]. The frequency bandwidth of speed controller is limited with ω_a and by setting k_{sp} (speed gain) to $(J_m+J_l)\omega_a$ we hope to reach the maximum achievable frequency bandwidth. Usually, in high stiff machine tools this frequency bandwidth reaches above 100HZ [21]. Simply for our study of mechanical vibration induced by backlash the current controller can be replaced by one. Then the transfer function of the speed controller can be given as (6a) where by increasing k_{sp} the dominant root of G_{sm} decreased from ω_r to ω_a. And for the frequency of much less than ω_a we can replace P and Q with one and (6a) reduces to (6b).

$$G_{sm}=\frac{\omega_m}{\omega_c}=\frac{(k_{sp}T_{si}s+1).P}{T_{si}(J_m+J_l)s^2Q+(k_{sp}T_{si}s+1).P} \tag{6a}$$

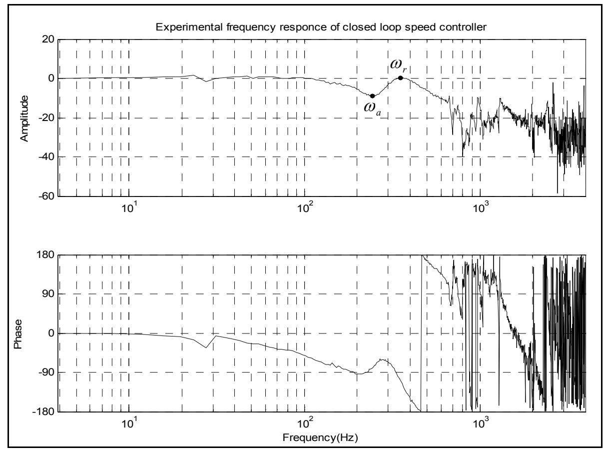

Fig. 2. Experimental frequency response of speed control of a milling machine tool

$$\frac{\omega_m}{\omega_c}=\frac{(k_{sp}T_{si}s+1)}{T_{si}(J_m+J_l)s^2+(k_{sp}T_{si}s+1)} \tag{6b}$$

Normally, $T_{si}(J_m+J_l)$ is much lees than one and for the frequency of mechanical vibration (6b) can be replaced with one. Fig.2 exemplifies the experimental frequency response of speed control of a machine tool. In practice, usually for the frequency of mechanical vibration(normally less than 30Hz) the speed controller can be replaced by 1(ideal speed control). In Fig.1 the high level position controller defines the speed set point of speed controller as (7). Using (6) and (7), the equation between motor speed and load positioning error can be given as (8). This equation restates (1).

$$\omega_c=k_v e_l \tag{7}$$

$$\frac{\omega_m}{e_l}=k_v \tag{8}$$

VI. FREQUENCY OF VIBRATION

During acceleration period, usually backlash gap is closed and the load-motor motion follows the dynamic of a rigid body. But the speed controller suffers backlash easily when speed is constant and any disturbance opens the gap and vibration may be resulted. Using Fast Fourier Transformation(FFT), the dominant frequency of such vibrations(that closely represents the real vibration) can be defined[6]. And the procedure of backlash detection can be reduced to the detection of estimated dominant frequency bandwidth from the current or speed signal spectrum.

To estimate the bandwidth of frequency in a high stiff servo axis, mechanical subsystem is considered as Fig.3. Movement of M_l (load) is controlled by the motion of M_m (motor) where they follow the pre described servo control(8). This system works based on the impact between M_m and M_l. Between each impact load moves freely with a constant speed(fiction is disregarded) and at the time of impact speed direction is reversed.

Impact nature is very complex event involving material deformation and recovery and heat-sound generation(energy loss). Though here a simple model of impact with a constant coefficient of restitution is incorporated, and the contact duration is neglected.

In Fig.3 at $t = 0$ load is at the center($x_l = 0$) and during the time before the coming impact:

$$0 \le t \le \frac{T}{4}, \dot{x}_l = const \tag{9}$$

Where T is the period of vibration. Using (8) and knowing the impact time($t = T/4$), the initial speed of driver at the time of contact would be:

$$\dot{x}_m = k_v \times x_l \Rightarrow \dot{x}_m = k_v . \dot{x}_l . \frac{T}{4} \tag{10}$$

The impact equation with the constant coefficient of restitution(e) is given by (11). Therefore, the relationship between k_v and the frequency of vibration($1/T$) can be achieved as (12).

$$\frac{\dot{x}_l - \dot{x}_m}{\dot{x}_l + \dot{x}_m} = e \tag{11}$$

$$f = \frac{1}{4} \times \frac{1+e}{1-e} k_v \tag{12}$$

In (12) the frequency of vibration is not affected by the magnitude of backlash, and it is proportional to the position control gain. This interesting fact was predicted by the sinusoidal-input describing function.

The coefficient of restitution for two steel balls in contact is about 0.6. And energy loss in a real impact between mechanical parts is high. So the frequency bandwidth of vibration in a servo axis can be approximated from (12) by varying e from 0 to 0.6 as:

$$k_v/4 \le f \le k_v \tag{13}$$

Fig.4 shows the experimental frequency of vibration obtained from six different machine tools and they all are in the bandwidth estimated by (13).

VII. Vibration Detection

Fig.5 shows the vibration detection approach in detail. The difference between the setting speed of interpolator and the output of position controller(command speed of (1)) is fed to vibration detector. The average for absolute values of "n+1" points is compared with their absolute value of average(in this paper "n" is 4). With a small enough sampling time(less than $(vibration\_period)/(2(n+1))$) peak points corresponding to the cross of the calculated speed

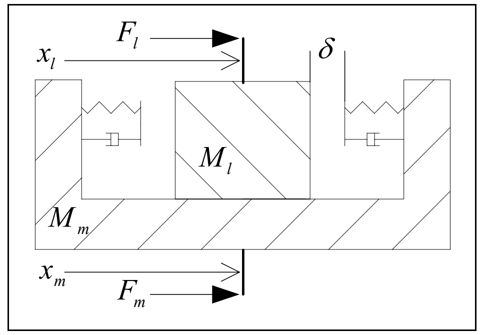

Fig. 3 Backlash simulation in a simple system

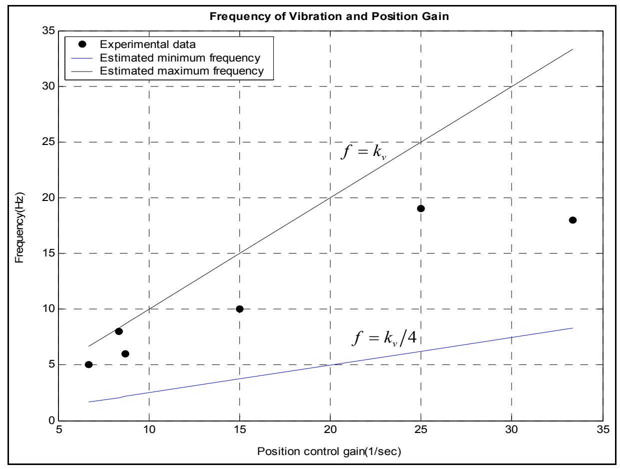

Fig. 4 Experimental frequency and estimated band width for 6 machine tools

with the reference speed are detected at the input of the holder in Fig.5. The nonlinear holding block holds the latest pick value unless the next cross happens. But the exact time and even occurrence of the next cross is not predictable. And in the case of stability there is no cross point(no vibration) while the holder gives the latest pick height. To adjust the condition, and to provide a time dependent parameter, at t_p (pick time) the output of holder multiplied with an exponentially decreasing function. If vibration disappears, the exponential function will bring the vibration level to zero in a limited time constant(T_v). This time can be offered as higher than five times of the period calculated by (13) as:

$$T_v \ge 5/f \tag{14}$$

At the end, a low pass filter(with time constant of T_f) is designed to produce smooth vibration level(β).

VIII. Backlash Suppression Approche

As mentioned before, backlash makes a delay between the turning of motor(driver) and the motion of axis(driven) that may lead to vibration. For the ordinary servo axis in Fig.1, load oscillation is multiplied by position gain and the result is fed to the speed control(ω_c). Then oscillation is

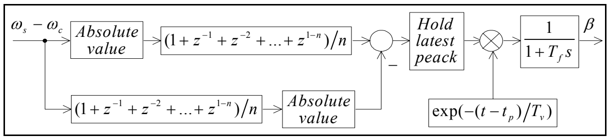

Fig. 5 Vibration detector

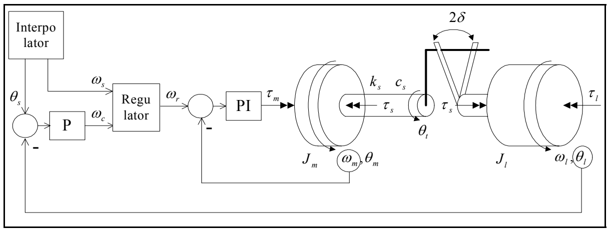

Fig. 6 Control system with integrated speed regulator

regenerated in the speed and current control and limit cycle is resulted.

To suppress the vibration, a specific, nonlinear speed regulator is integrated in Fig.6. Based on the vibration level(β), the regulating-switching factor(λ) and regulated speed(ω_r) are defined by (15):

$$\begin{aligned} &\lambda = exp(-\beta/\beta_T) \\ &\omega_r = \omega_s - \lambda(\omega_s - \omega_c) \end{aligned} \tag{15}$$

Where β_T is the vibration threshold. This threshold should be defined experimentally by starting from small values for stability, and it is increased to improve the response. In the case of vibration, regulation factor in (15) became zero and the effect of load sensor(oscillatory part) on regulated speed is eliminated. Then stability with the cost of some following error is resulted. When stability is detected switching factor converges to one, and the load sensor is included in the speed regulator then exactness is satisfied.

IX. Axis Modeling

Machine tools of TUGA company are in production and warranty period so there is no opportunity for experimental results. For this reason a real linear axis(motor, ball screw, guide ways and carriage) of a high performance milling machine is modeled. Some control parameters defined in machine data are: $k_v = 25(s^{-1})$, $k_{sp} = 52(Nm.s/rad)$, $T_{si} = 7.5ms$, $J_m = 0.0625(Kg.m^2)$, $k_r = 100\pi$. Screw mass moment of inertia was calculated as $J_{screw} = 0.0784Kg.m^2$. Unknown mechanical parameters(load mass moment of inertia, reflected friction torque on motor) were optimized by Nelder-Mead simplex algorithm. Total number of 1600 points from experimental servo trace at 2.5 ms sampling time are used and the results are: $M_l = 6554.2Kg$, $\tau_f = 1.2sign(v_l) + 57.3v_l$. Anti-resonance frequency(then stiffness) was estimated through the experimental frequency response like Fig.2 as $\omega_a = 600rad/s$. Then model is

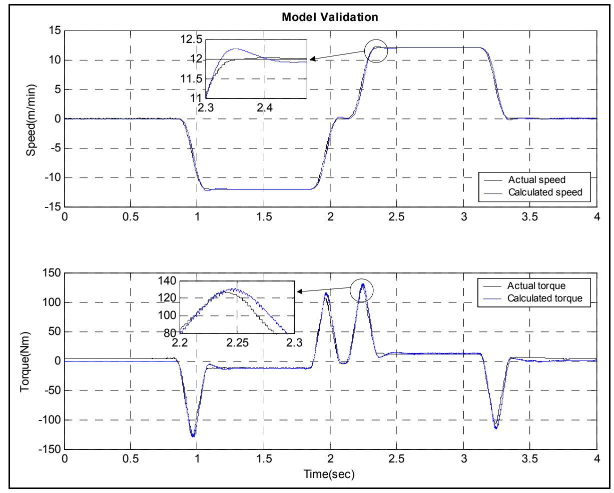

Fig. 7 Model validation for the speed step change. A: Axis speed comparision, B: Motor torque comparision.

validated in Fig.7 by the closeness of response of the real axis and the model for input of speed step change.

X. Simulation

Fig. 8, 9 simulate response and performance of the optimized model with the ordinary control system(Fig.1) and with integrated speed regulator(Fig.6) where input is speed step change and $\delta = 0.1(mm)$. To simulate the real condition a step disturbance force of 6280(N)(it's reflection on the motor torque is 20(Nm)) was applied to the load side from 2(s) to 4(s). The torque was applied in the direction of motion to open the backlash gap and to make the condition more critical. In Fig. 8 and 9, part **A** compares the calculated following error in (1) with motor-load following error. Part **B** illustrates the disturbance torque and part **C** shows the vibration level. Finally, part **D** exposes the regulation factor. In Fig.8 the remarkable disturbance closes the backlash gap firmly and motion becomes smooth. However, as the disturbance torque is eliminated, because of friction, the direction of the net force on the load side is reversed. Then backlash gap opens and the system starts to oscillate for the rest of motion. In comparison, Fig.9 shows the efficiency of regulator for backlash suppression(smooth motion) even with the presence of disturbance. It also reveals the exactness of system for both tracking of desired dynamic error and stand still positioning(part A of Fig.9).
It should be mentioned that this regulator is ideal for positioning axes where standstill positioning and smooth motion are of most interest(not the dynamic following error). ***And some advantages of the proposed regulator are routine tuning, integration with the original controller and its impressive performance with unknown backlash.***

XI. Conclusion

Using simple models for the mechanical subsystem, and backlash itself the frequency of vibration in a servo axis is estimated. It was shown that the frequency of vibration is not affected by the magnitude of backlash while it is the

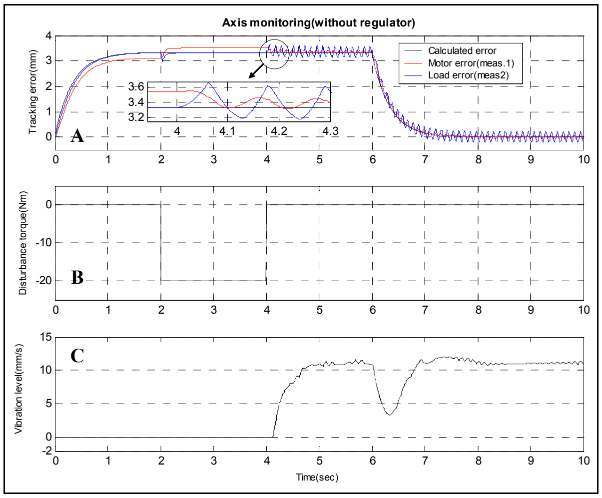

Fig. 8 Axis(model) monitoring without regulator. A: Following error, B: Disturbance torque, C: Vibration level.

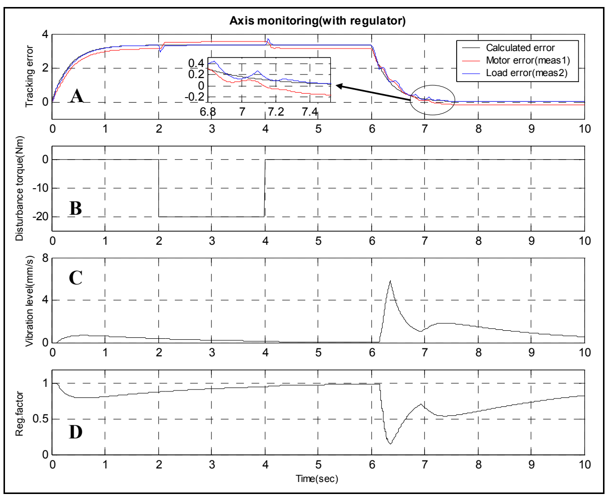

Fig.9. Axis(model) monitoring with regulator. A: Following error, B: Disturbance torque, C: Vibration level, D: Regulating factor.

position control gain that dictates this frequency. This fact is in accordance with the result of describing function theory. Vibration detection and knowledge of the frequency of vibration in a servo axis are significantly helpful for condition monitoring and preventive maintenance. In addition, designing the speed regulator enables control system to efficiently suppress the unknown backlash and eliminates the vibration. The regulator also procures the exact stand still positioning and full fills the calculated dynamic following error in (1) for the ordinary control system.

REFERENCES

[1] S. Dubowsky and F. Freudenstein. "Dynamic analysis of system with clearance, Part1 and 2." *ASME Journal of Engineering for Industry, 93:305-316, February 1971*.

[2] W. Goldsmith. "IMPACT, The Theory and Physical Behavior of Colliding Solids," Edward Arnold, London, 1960.

[3] Gerdes, J.C., and Kumar, V., "An impact model of mechanical backlash for control system analysis," *Proceedings of the American Control Conference,* Volume 5, 21-23 June 1995, pp. 3311-3315.

[4] Tore Hagglund, "Automatic on-line estimation of backlash in control loops," *Journal of Process Control 17 (2007) 489-499.*

[5] Christopher K. Halse, R. Eddie Wilson, Mario di Bernardo and Martin E. Homer, "Coexisting solutions and bifurcations in mechanical oscillator whith backlash," Journal of Sound and Vibration 305 (2007) 854-885.

[6] Moosavian, S. Ali A. and MohammadiAsl, Ebrahim, "Backlash Detection in CNC Machines Based on Experimental Vibration Analysis," IEE *International Conference on* Robotics, Automation and Mechatronics, Volume , Issue , 21-24 Sept. 2008 Page(s):393 – 398, Digital Object Identifier 10.1109/RAMECH.2008.4681515.

[7] Nordin, M. (1995), "Uncertain systems with backlash: Analysis, identification and synthesis," *Licenciate thesis, trita/mat-95-os3, Royal Institute of Technology.*

[8] Lagerberg, Adam, "A literature survey on control of automotive *powertrains* with backlash," *Jönköping University*, report, 2001.

[9] Nordin M., Gutman., "Controlling mechanical systems with backlash- a survey," *Automatica,* vol.38, pp. 1633-1649**,** October 2002.

[10] Koyama, M., & Yano, M. (1991), "Two degrees of freedom controller using reference system model for motor drives," *Proceedings of the European conference on power electronics and applications*, Firenze (pp. 596–602). Firenze, Italy: EPE.

[11] Brandenburg, G., and Sch¨afer, U., "Influence and partial compensation of simultaneously acting backlash and Coulomb friction in a position- and speed-controlled elastic two-mass system", *Proc 2nd European Conf. on Power Electronics and Applications.*, EPE, Grenoble, 1041-1047, (1987).

[12] Brandenburg, G., "Stability of a speed controlled elastic two-mass system with backlash and Coulomb friction and optimization by a disturbance observer, " *Proceeding of the IMACS Conference on Applied Modelling and Simulation of Technological Systema,* (pp. 371-381).

[13] Hori, Y.,H. Iseki and K.Sugiura (1994)," Basic consideration of vibration suppression and disturbance rejection control of multi-inertia system using SFLAC(state feedback and load acceleration control)," *IEEE Transaction onIindustry Application*s. 30(4): 889-896.

[14] Odai, M. Hori, Y. (1998), "Speed control of 2-inertia system with gear backlash using gear torque compensator," *Proceeding of the IEEE Industrial Workshop on Advanced Motion Control,* (pp.234-239).

[15] H. Ikeda, M. Koyama, "Performance analysis of mechanical vibration suppression control system for motor drives with elastic load based on frequency response," *Proceedings of the IEEE InernationalConference on Industrial Technology, 1996.*

[16] Y. Hori, H. Sawada, "Slow resonance ratio control for vibration suppression and disturbance rejection in torsional system," *IEE Trans. IE, vol.46, No.1, pp.162-168, Feb. 1999.*

[17] Slobodan N. Vukosavic, Milic R. Stojic, "Suppression of torsional oscillation in a high-performance speed servo drive," *IEEE Transactions on Industrial Electronics, Vol. 45, No. 1, Feb 1998.*

[18] Masahiko ITOH, "Suppression of transient vibration for geared mechanical system with backlash using model-based control," *JSME International Journal, Series C, Volume 47, No.1, 2004.*

[19] Stein, J. L., and Wang, C. H., "Automatic detection of clearance in mechanical systems: theory and simulation," Proceedings of the American Control Conference, Volume 3, 21-23 June 1995, pp. 1737-1745.

[20] Lagerberg, A., and Egardt, B., "Backlash Estimation With Application to Automotive Power trains," *IEEE Transactions on Control Systems Technology*, Volume 15, Issue 3, May 2007, pp. 483-493.

[21] Simens simodrive 611 digital/SINUMERIC840D/810D startup and optimizationoptimization.